frontiers in Chemistry

ORIGINAL RESEARCH
published: 20 January 2022
doi: 10.3389/fchem.2021.840446

Efficient Sorption of Arsenic on Nanostructured Fe-Cu Binary Oxides: Influence of Structure and Crystallinity

Gaosheng Zhang, Zhijing Wu, Qianying Qiu and Yuqi Wang**

Key Laboratory for Water Quality and Conservation of the Pearl River Delta, School of Environmental Science and Engineering, Ministry of Education, Guangzhou University, Guangzhou, China

To study the structure-performance relationship, a series of nanostructured Fe-Cu binary oxides (FCBOs) were prepared by varying synthesis conditions. The obtained binary oxides were well characterized using X-ray diffraction (XRD), transmission electron microscope (TEM), Brunner-Emmet-Teller (BET), magnetic and Zeta potential measurement techniques. Both As(V) and As(III) sorption on the FCBOs were evaluated by batch tests. Results show that the surface structure and crystallinity of FCBOs are greatly dependent on preparation conditions. The crystallinity of FCBOs gradually increases as the synthesis pH value increasing from 9.0 to 13.0, from amorphous phase to well-crystalline one. Simultaneously, the morphology change of FCBOs from irregular agglomerate to relatively uniform polyhedron has been observed. The sorption of arsenic is greatly influenced by the crystallinity and structure of FCBOs, decreasing with increasing degree of crystallinity. The amorphous FCBO has higher surface hydroxyl density than well-crystalline one, which might be the reason of higher sorption performance. As(V) is sorbed by the FCBOs via formation of inner-sphere surface complexes and As(III) is sorbed through formation of both inner- and outer-sphere surface complexes. This investigation provides new insights into structure-performance relationship of the FCBO system, which are beneficial to develop new and efficient sorbents.

Keywords: Fe-Cu binary oxide, arsenic, sorption, structure-performance relationship, crystallinity

OPEN ACCESS

Edited by:
Qingyi Zeng,
University of South China, China

Reviewed by:
Jingyang Luo,
Hohai University, China
Xia Ligang,
Shanghai University of Electric Power, China

****Correspondence:***
Gaosheng Zhang
gszhang@gzhu.edu.cn
Yuqi Wang
yqwang@gzhu.edu.cn

Specialty section:
This article was submitted to Inorganic Chemistry, a section of the journal Frontiers in Chemistry

Received: *21 December 2021*
Accepted: *31 December 2021*
Published: *20 January 2022*

Citation:
Zhang G, Wu Z, Qiu Q and Wang Y (2022) Efficient Sorption of Arsenic on Nanostructured Fe-Cu Binary Oxides: Influence of Structure and Crystallinity. Front. Chem. 9:840446. doi: 10.3389/fchem.2021.840446

INTRODUCTION

Arsenic contamination has emerged as one of global environmental issues in the last decades due to its high toxicity (Smedley and Kinniburgh, 2002). In natural waters, arsenic exists mainly in two inorganic forms as arsenate [As(V)] and arsenite [As(III)]. In view of the serious adverse effects of arsenic, a number of treatment techniques such as coagulation/precipitation, ion exchange, adsorption, membrane filtration and biological treatment, have been exploited for arsenic removal from drinking water and wastewater. Among them, adsorption is commonly and extensively used, due to its simplicity in operation, high efficiency and cost-effectiveness (Mohan and Pittman, 2007; Hu et al., 2015). Various adsorbents have been developed and used for arsenic removal (Mohan and Pittman, 2007). Recently, metal (hydr)oxides such as Fe (hydr)oxides (Sowers et al., 2017; Usman et al., 2020), feroxyhyte (Usman et al., 2021), Al oxides (Han et al., 2013; Mertens et al., 2016), TiO_2 (Guan et al., 2012; Yan et al., 2015), ZrO_2 (Hristovski et al., 2008; Cui et al., 2012; Shehzad et al., 2019), CeO_2 (Srivastava, 2010; Li et al., 2012), CuO

(Martinson and Reddy, 2009; Yu et al., 2012; Reddy et al., 2013) etc., have attracted considerable attention because they exhibit strong sorption properties towards arsenic.

More recently, composite sorbents containing two or more metal oxides have been emphasized for their enhanced sorption performance and synergistic effect. For example, an Fe-Mn binary oxide prepared by Zhang and coworkers demonstrates a greater enhancement in both As(V) and As(III) removal (Zhang et al., 2014); amorphous Fe-Ti bimetal oxides synthesized by Rao and coworkers have higher performance in both As(V) and As(III) removal than pure component oxides (Rao et al., 2015); a Ce-Mn binary oxide synthesized by Chen and coworkers exhibits higher arsenic removal efficiency than parent oxides (Chen et al., 2018); an Fe-Ni-Mn trimetal oxide reported by Nasir and coworkers is found to be efficient for As(III) removal (Nasir et al., 2018); an Fe-Cu-Mn trimetal oxide fabricated by Zhang and coworkers displays high sorption capacity for both As(V) and As(III) (Zhang et al., 2020).

Many literatures demonstrated that the sorption ability of metal oxides was strongly affected by their structure and crystallinity. Therefore, it is very necessary to study systemically the structure-performance relationship of synthesized metal oxides. Some researchers have investigated this relationship of single metal oxide system (Jegadeesan et al., 2010; Dou et al., 2016). However, very few researches have been done about binary metal oxide systems (Dou et al., 2018). In our previous study, a novel amorphous Fe (III)-Cu (II) binary oxide prepared with a Cu/Fe molar ratio of 1:2 was found to have high sorption ability towards arsenic (Zhang G et al., 2013). Moreover, it was superior to its parent components (ferrihydrite and cupric oxide) and crystalline $CuFe_2O_4$ (Tu et al., 2012; Wei et al., 2019). This Fe(III)-Cu(II) binary oxide system is very interesting because it can exist as a pure compound of $CuFe_2O_4$ or a mixture of ferrihydrite and cupric (hydr)oxide, depending on preparation conditions (Tu et al., 2012; Zhang G et al., 2013), which is very different from other binary systems (Zhang et al., 2014; Rao et al., 2015). Therefore, to investigate the structure-performance relationship of Fe(III)-Cu(II) binary oxide system is very vital, which will facilitate further understanding the arsenic sorption behaviors on binary oxide system and developing new composite adsorbents. To our best knowledge, until now, no information about the structure-performance relationship of Fe (III)-Cu (II) binary oxide is available in literatures.

Therefore, the main objectives of this study are 1) to synthesize a series of Fe-Cu binary oxides with different structure and crystallinity degree by varying the synthesis solution pH; 2) to characterize the morphology and crystallinity of as-synthesized binary oxides using a variety of techniques; 3) to evaluate the arsenic adsorption behavior and performance of binary oxides by batch tests; and finally 4) to investigate the structure-performance relationship of Fe-Cu binary oxide system.

MATERIALS AND METHODS

Materials

Analytical grade chemicals including $FeCl_3.6H_2O$, $CuSO_4.5H_2O$ and NaOH were purchased from Sinopharm Chemical Reagent Beijing Co., Ltd. (Beijing, China). They were directly used and no further purification was done. As (V) and As (III) stock solutions were prepared with deionized water using $Na_2HAsO_4.7H_2O$ and $NaAsO_2$, respectively. Arsenic working solutions were freshly prepared by diluting stock solutions with deionized water. Glass vessels were used as reactors. Before use, reactors were firstly cleaned using 1% HNO_3 solution and then washed several times with deionized water.

Preparation of Fe-Cu Binary Oxides (FCBOs)

A series of FCBOs with a Fe/Cu molar ratio of 2:1 were prepared at different pHs, according to a slightly modified method described by Zhang G et al. (2013). Specifically, about 10.8 g ferric chloride hexahydrate ($FeCl_3.6H_2O$) and 5.0 g copper (II) sulfate pentahydrate ($CuSO_4.5H_2O$) were dissolved in 400 ml deionized water. Under vigorous mechanical-stirring, NaOH solution (3 M) was added dropwise to raise the pH of mixture to a predetermined value (9.0 or 11.0 or 12.0 or 13.0). The formed suspensions were continuously stirred for 0.5 h, aged at 100°C for 6 h using a hot water bath. After cooling, the prepared suspensions were washed several times with distilled water. Afterwards, they were treated by filtration and dried at 55°C for about 24 h. The dried FCBOs were crushed into fine powders (0.5–50 μm) and stored in a desiccator. According to the synthesis pH value, these FCBOs are denoted as FC1, FC2, FC3, and FC4, respectively.

Characterization of FCBOs

X-ray diffraction analyses were performed on a Rigaku D/Max-3A diffractometer using Ni-filtered copper Kα one radiation (XRD, Rigaku, Japan). The morphology of FCBOs was analyzed using a transmission electron microscope (TEM, Hitachi H-800, Japan). Specific saturation magnetization (M_s) and magnetization remanence (M_r) measure of particles' magnetism, was determined using vibrating sample magnetometer at room temperature (VSM, Model 7,307 Lakeshore, United States). Specific surface area was determined by nitrogen adsorption (BET-method) using a surface area analyzer (Nova 2000e; Quantachrome Instruments, United States). A zeta potential analyzer (Zatasizer 2000; Malvern, UK) was used to analyze zeta potential of the FCBOs.

The density of surface hydroxyl sites was determined by a surface titration method (Dou et al., 2016). Fe-Cu binary oxide (0.3000 g) was added into 50 ml of 0.05 mol/L NaOH solution. Its accurate molar concentration was titrated using a 0.0500 mol/L Na_2CO_3 solution-calibrated HCl solution (0.0502 mol/L). After 4 h shaking at 130 rpm with the temperature maintained at 25°C, the mixture solution was passed through a 0.45 μm membrane. The filtrate was titrated using the HCl solution and residual NaOH in it was neutralized until pH up to 7.0, then the amount of surface hydroxyl can be calculated based on the amount of NaOH consumed.

Batch Sorption Experiments

A series of batch experiments were performed to investigate the sorption of arsenic on FCBOs. A certain amount of FCBO was put

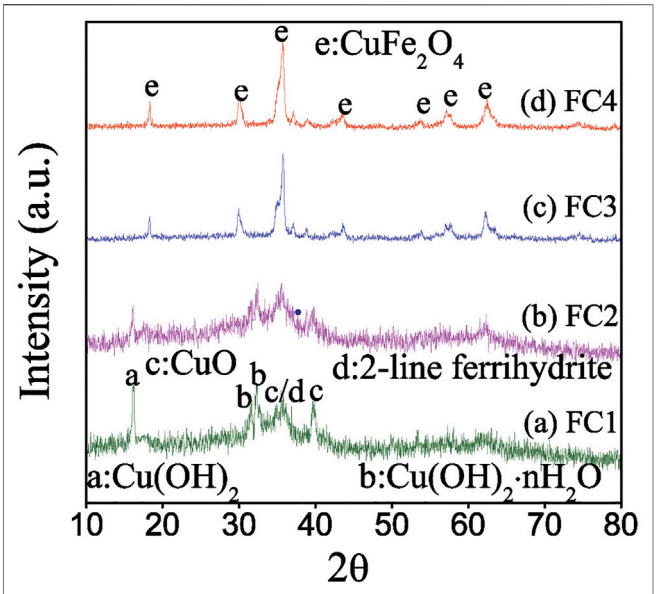

FIGURE 1 | X-ray diffraction patterns of the Fe-Cu binary oxides: (a) FC1, (b) FC2, (c) FC3 and (d) FC4. (a: $Cu(OH)_2$, b: $Cu(OH)_2{\cdot}nH_2O$, c: CuO, d: 2-line ferrihydrite and e: $CuFe_2O_4$).

into 100 ml glass vessels containing 50 ml arsenic solution of different concentrations. The vessels were then oscillated on a shaker at 170 rpm for 24 h. After reaction, all samples collected were filtrated using 0.45 μm membrane and then were analyzed for arsenic. More detailed description of sorption experiments can be seen in the Supplementary Material.

Analytical Methods

Prior to arsenic analysis, the aqueous samples were diluted to a concentration below 100 μg/L, acidified with concentrated HNO_3, and stored in acid-washed glass vessels. Arsenic concentration was determined using an inductively coupled plasma mass spectrometry machine (ICP-MS, ELAN DRC II, Perkin Elmer Co. United States).

RESULTS AND DISCUSSION

Properties of the FCBOs

X-ray diffraction patterns of the as-prepared FCBOs are presented in **Figure 1**. For FC1, five broad peaks at approximately 16.2, 31.7, 32.3, 35.8 and 39.8° are observed. The characteristic peak at 16.2° belongs to the copper hydroxide ($Cu(OH)_2$) (JCPDS 80-0656); the peaks at 31.7 and 32.3° are attributed to the hydrated copper hydroxide ($Cu(OH)_2{\cdot}nH_2O$) (JCPDS: 42-0638); the peak at 35.8° might be ascribed to both copper oxide (CuO) (JCPDS: 45-0937) and 2-line ferrihydrite formation (Hofmann et al., 2004); the peak at 39.8° might belong to the CuO (JCPDS: 45-0937). Obviously, the FC1 exists mainly as an amorphous mixture of 2-line ferrihydrite and copper (hydr)oxides. The X-ray diffraction pattern of FC2 is closely similar to that of FC1. However, the intensity of peaks belonging to copper hydrated hydroxide, hydroxide and oxide decreases with an increase in synthesis pH value. When the synthesis pH reaches 12.0 (FC3), these peaks disappear almost completely, and new diffraction peaks appear at 18.3, 30.0, 35.8, 43.6, 53.7, 57.8 and 62.4°, respectively. These characteristic peaks are attributed to the well-crystalline copper ferrite ($CuFe_2O_4$) (JCPDS: 34-0425). With a further increase in synthesis pH value from 12.0 to 13.0 (FC4), the intensity of these peaks increases, indicating a greater crystallinity.

Transmission electron micrographs (TEMs) of the FCBOs are shown in **Figure 2**. It can be seen that the FCBO particles produced at pH 9.0 (FC1, **Figure 2A**) are agglomerates of smaller nanoparticles. The morphology of FC2 (**Figure 2B**) is very similar to that of FC1. When the synthesis pH increases from 11.0 to 12.0, the major of amorphous particles (FC3, **Figure 2C**) becomes crystallized grains with visible grain boundaries and polyhedron shapes. For FC4 (**Figure 2D**), much more uniform grains are observed, suggesting well-crystalline $CuFe_2O_4$ particles are dominant under this condition. These results agree with those of XRD analysis.

The magnetic hysteresis curves of FCBOs are depicted in **Figure 3**. The hysteresis loops of FC3 and FC4 show a normal *S*-shape type, while those of FC1 and FC2 exhibit a nonhysteresis straight line, indicating that they are paramagnetic or superparamagnetic. The parameters of magnetic properties are summarized in **Table 1**. It can be seen that the saturation magnetization (M_s) increases with increasing synthesis pH value. For FC1 and FC2, they demonstrate very weak magnetism and the value of saturation magnetization is less than 0.4 emu/g. As the synthesis pH increases from 11.0 to 12.0, the saturation magnetization of FC3 rises sharply to 19.5 emu/g, which is far higher than that of FC2 and is very close to the $CuFe_2O_4$ nanoparticle (20.6 emu/g) synthesized via citrate-nitrate combustion method (Anandan et al., 2017). The magnetism of FC4 is the strongest and the saturation magnetization is as high as 26.9 emu/g. These results indicate that the magnetic properties of the FCBOs are closely related to their crystallinity.

The results of BET surface area measurements of the FCBOs are listed in **Table 1**. It can be clearly seen that the BET surface area of FCBOs decreases gradually with an increase in synthesis pH value. The BET surface area of FC1 is 268 m^2/g. However, the surface area of FC4 is only 90 m^2/g. It seems that the BET surface area of FCBOs is inversely proportional to its crystallinity.

Sorption Envelope

The influence of solution pH on arsenic sorption was investigated and the results are shown in **Figure 4**. For all FCBOs, the sorption of As (V) depends evidently on solution pH value. The greatest sorption occurs under acidic conditions and decreases with increasing solution pH, which is a typical characteristic for anions sorption by metal oxides and oxyhydroxides (Ren et al., 2011; Jordan et al., 2014). Over the tested pH range (3.0–11.0), As(V) mainly exists as negatively charged $H_2AsO_4^-$ and $HAsO_4^{2-}$ in water (pKa of dissociation is 2.20, 6.97 and 11.53, respectively). Under weak acidic conditions, the surface of the FCBO is positively charged because of protonation and $H_2AsO_4^-$ is dominant species in aqueous solution, which is beneficial for electrostatic attraction between the surface of FCBO and the

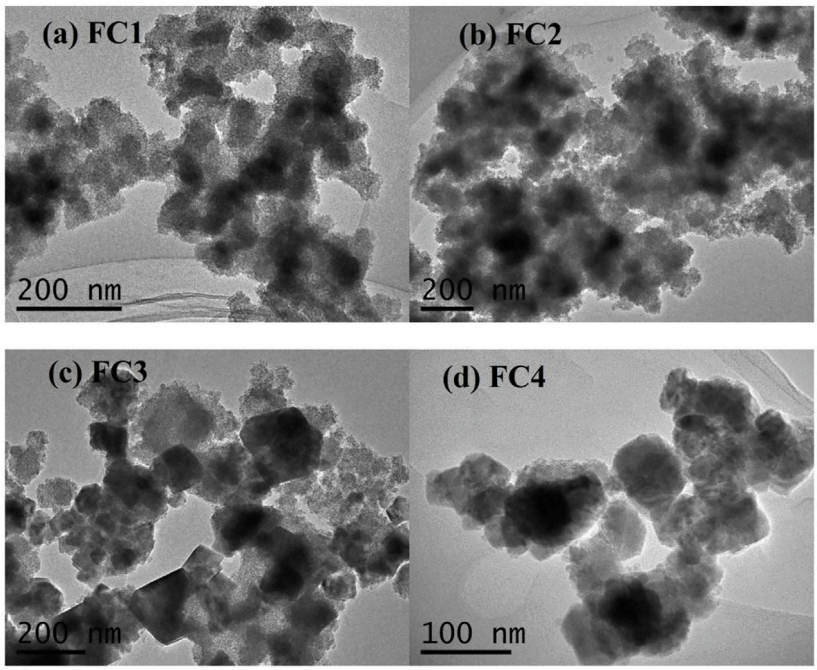

FIGURE 2 | TEM images of the Fe-Cu binary oxides: **(A)** FC1, **(B)** FC2, **(C)** FC3 and **(D)** FC4.

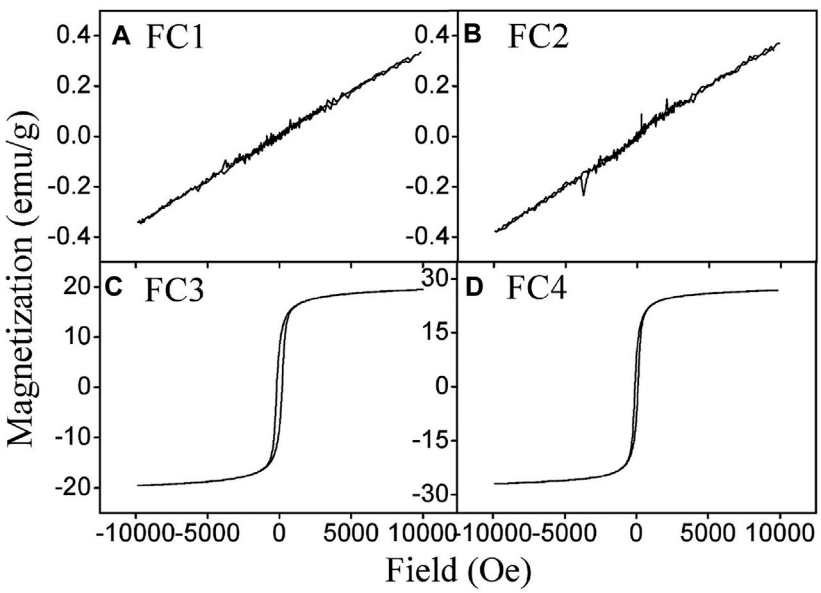

FIGURE 3 | Magnetization loops of the prepared Fe-Cu binary oxides: **(A)** FC1, **(B)** FC2, **(C)** FC3 and **(D)** FC4.

aqueous $H_2AsO_4^-$. With an increase in solution pH, the surface of FCBO becomes less positively charged and even negatively charged. At the same time, $HAsO_4^{2-}$ (a more negatively charged As (V) species) becomes to be dominant. Therefore, the attraction between the surface of FCBO and As (V) species weakens and as a consequence, As (V) sorption decreases.

Compared to As (V), the influence of solution pH on As (III) sorption is markedly different. Its sorption enhances gradually as solution pH increases and a maximum sorption occurs at about pH 9.1. Afterwards, further increase in pH decreases the sorption of As (III). Similar phenomena have been reported for the As (III) sorption by other binary metal oxides (Ren et al.,

TABLE 1 | Saturation magnetization and BET specific surface area of the as-prepared Fe-Cu binary oxide samples.

Samples	Synthesis pH	Saturation magnetization (emu g^{-1})	Specific surface area (m^2 g^{-1})
FC1	9.0	0.34	268
FC2	11.0	0.37	202
FC3	12.0	19.52	130
FC4	13.0	26.88	90

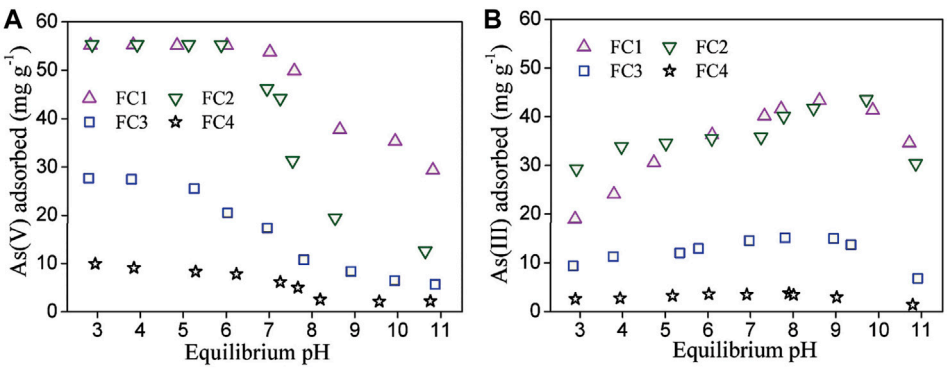

FIGURE 4 | Effect of solution pH on **(A)** As (V) and **(B)** As (III) sorption by Fe-Cu binary oxides. Initial arsenic concentration = 11.0 mg/L, adsorbent dose = 200 mg/L and T = 25 ± 1°C.

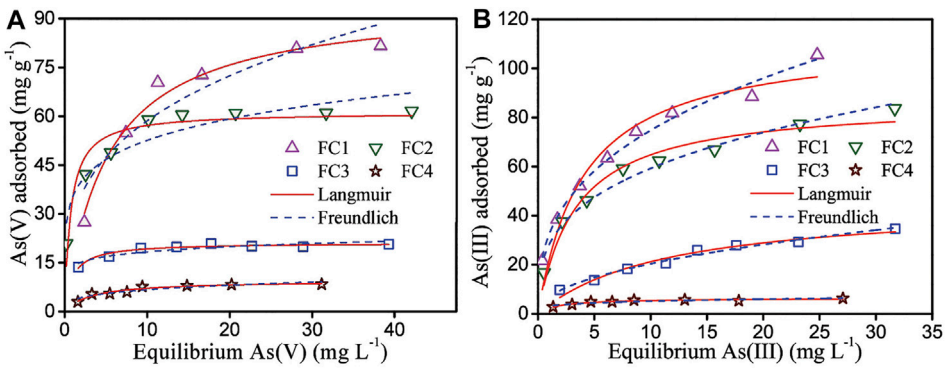

FIGURE 5 | Adsorption isotherm of **(A)** As (V) and **(B)** As (III) by Fe-Cu binary oxides. Initial arsenic concentration = 2–60 mg/L, adsorbent dose = 200 mg/L, pH = 7.0 ± 0.1 and T = 25 ± 1°C.

2011). Generally, a maximal sorption of weak acid anions onto metal oxides occurs at pH values close to pk_{a1} of the acid. The pk_{a1} of H_3AsO_3 is 9.2. The reduction in As (III) sorption at pH above 9.1 may be ascribed to the Coulombic repulsion between the negative surface of FCBOs (pH_{pzc} = 7.3-9.0) and negatively charged As (III), whereas the predominant form of As (III) species is $H_2AsO_3^-$.

Sorption Isotherm

The sorption isotherms of arsenic on the FCBOs are depicted in **Figure 5**. Obviously, the sorption of arsenic by the FCBO is closely related with its crystallinity. The FC1 has the strongest uptake ability for both As(V) and As(III) and the maximum sorption capacities are 83.3 and 112.2 mg/g at pH 7.0 (Langmuir model), respectively. The arsenic uptake ability of FCBOs decreases in the following order: FC1>FC2>FC3>FC4. Furtherly, the maximum sorption capacities of FC1 and FC2 are far larger than those of FC3 and FC4. The sorption performance of metal oxides depends generally on their surface area. However, the decrease in arsenic uptake by the FCBOs is not completely proportional to the reduction of specific surface area. This can be explained as follows. The specific surface area of the FCBOs is determined by N_2 molecule, which is smaller than the arsenic molecule. Partial surfaces of the FCBOs are inaccessible to arsenic molecule. Additionally, the As(V) and As(III) maximal sorption capacities

TABLE 2 | Langmuir and Freundlich isotherm parameters for As (V) and As (III) adsorption on Fe-Cu binary oxides at pH 7.0 ± 0.1.

Adsorbent	As species	Langmuir model			Freundlich model		
		q_{max} (mg/g)	K_L (L/mg)	R^2	K_F ($mg^{1-1/n}L^{1/n}g^{-1}$)	1/n	R^2
FC1	As(V)	83.3	0.19	0.977	58.9	0.31	0.844
FC2	As(V)	61.3	1.40	0.900	35.5	0.17	0.884
FC3	As(V)	21.1	1.03	0.935	14.0	0.12	0.806
FC4	As(V)	9.5	0.31	0.935	3.5	0.28	0.842
FC1	As(III)	112.2	0.25	0.936	32.6	0.36	0.988
FC2	As(III)	86.5	0.30	0.961	28.4	0.32	0.974
FC3	As(III)	45.3	0.09	0.959	6.9	0.47	0.980
FC4	As(III)	6.4	0.55	0.920	3.1	0.22	0.819

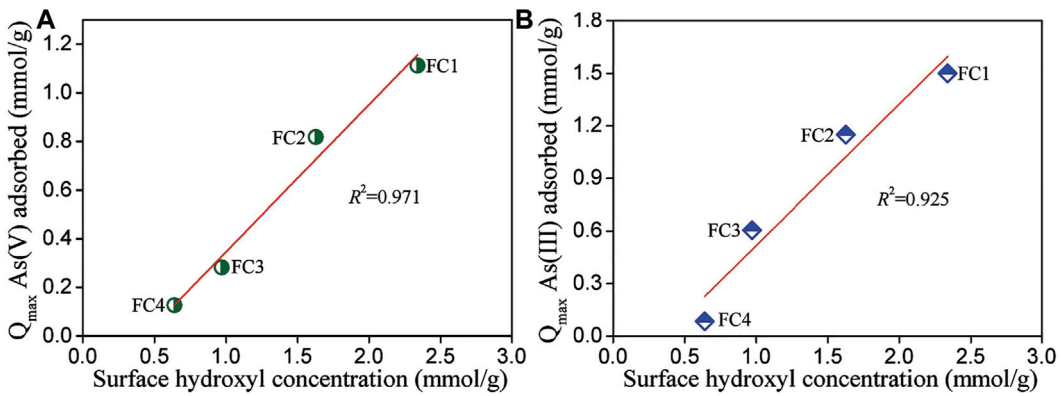

FIGURE 6 | Relationship between surface hydroxyl concentration and **(A)** As (V) and **(B)** As (III) adsorption capacities of Fe-Cu binary oxides.

of Fe-Cu binary oxide synthesized at pH 7.5 are 82.7 and 122.3 mg/g, respectively (Zhang G et al., 2013). Obviously, the arsenic sorption ability of FC1 is to very close to that of Fe-Cu binary oxide prepared under neutral condition.

Both Langmuir and Freundlich models (seen in the Supplementary Material) were employed to fit the isotherm data. The fitting results and obtained parameters are shown in **Figure 5** and **Table 2**, respectively.

For As (V), the Langmuir model is more favorable for fitting the data, giving higher correlation coefficients (R^2). However, the Freundlich model is more suitable to describe the adsorption of As(III) on Fe-Cu binary oxides except for FC4, according to the correlation coefficients. The As (V) adsorption is likely a monolayer adsorption because the Langmuir model supposes that the adsorption process is a monolayer adsorption. While As (III) adsorption is a multilayer adsorption since the Freundlich model presumes that adsorption occurs on the heterogeneous surface and follows multilayer adsorption.

Relationship Between Surface Hydroxyl Concentration and Arsenic Adsorption Capacity

The surface of metal oxides in water is easily hydroxylated, due to the dissociation of chemisorbed water molecules, and the formed surface hydroxyl groups are responsible for anions adsorption from water by the exchange with hydroxide ions (Tamura et al., 1999). To reveal the relationship between surface hydroxyl concentration and arsenic adsorption capacity of FCBOs, the amounts of surface hydroxyl groups were determined by titration method and the results are demonstrated in **Figure 6**. It can be seen that FC1 has the largest amount of surface hydroxyl groups per unit weight (2.34 mmol/g), followed by FC2 (1.63 mmol/g), FC3 (0.97 mmol/g), and FC4 (0.64 mmol/g). Evidently, surface hydroxyl concentration of FCBO is negatively correlated with its crystallinity. However, arsenic sorption capacity of FCBO is well positively correlated with its surface hydroxyl concentration. The data was fitted using a linear equation and the coefficient of determination (R^2) of linear regression for As (V) and As(III) is 0.971 and 0.925, respectively. It should be noted that the intercept is negative, indicating that not all surface hydroxyl groups are efficient for arsenic, especially for FCBO with high crystallinity. This could be explained as follows. The space structure of arsenic species ($H_2AsO_4^-$, $HAsO_4^{2-}$ or H_3AsO_3) is remarkably larger than that of hydrogen ions, which was used to determine the amounts of surface hydroxyl groups. Therefore, partial hydroxyl groups on the surfaces could not be available for the arsenic molecules. To some extent, the arsenic sorption capacity of FCBO could be evaluated by the amounts of surface hydroxyl groups.

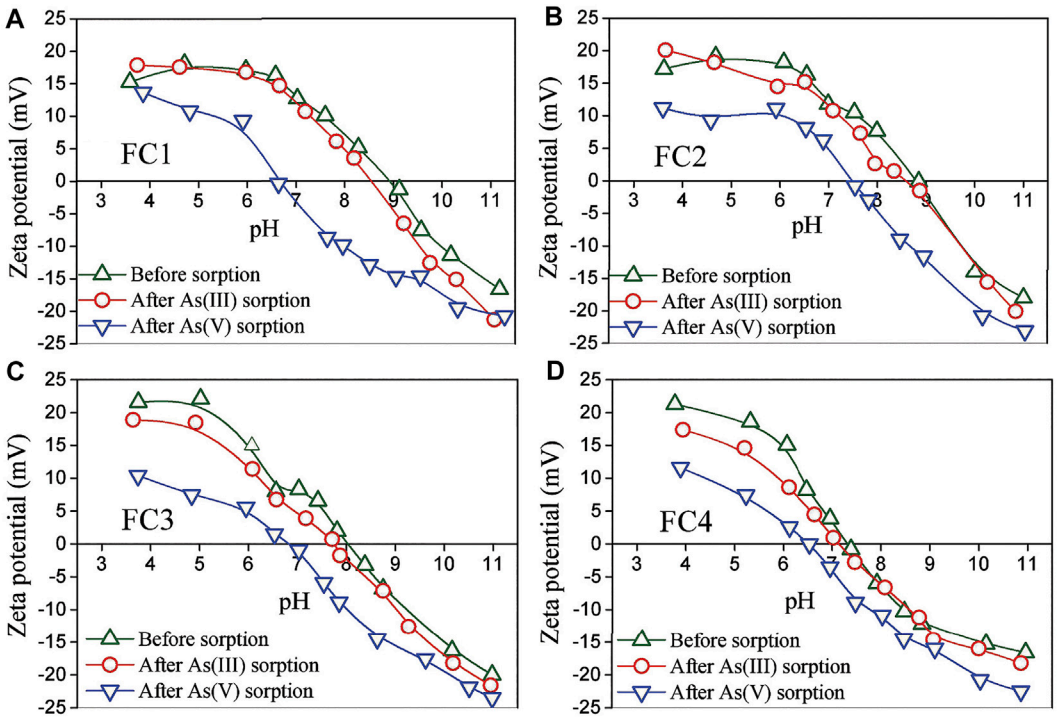

FIGURE 7 | Zeta potential of Fe-Cu binary oxides before and after arsenic adsorption. Initial arsenic concentration = 10 mg/L, adsorbent dose = 200 mg/L, ionic strength = 0.01 M $NaNO_3$, equilibrium time = 72 h.

Zeta Potential and FTIR Analysis Before and After Arsenic Adsorption

The zeta potentials of synthesized Fe-Cu binary oxides before and after reaction with arsenic were measured. As presented in **Figure 7**, the pH_{pzc} (pH at point of zero charge) of the virgin FC1, FC2, FC3 and FC4 were about 9.0, 8.8, 8.1 and 7.3, respectively. Evidently, the pH_{pzc} of the FCBOs decreases with increasing in crystallinity. This could be explained as follows. The pH_{pzc} values of CuO and $Cu(OH)_2$ are commonly over 9.2 (Martinson and Reddy, 2009; Kosmulski, 2009; Yu et al., 2012), and the pH_{pzc} of amorphous ferrihydrite is mostly in the range of 7.6–8.7 (Kosmulski, 2009; Antelo et al., 2010). As a mixture of these compounds, the amorphous FC1 and FC2 show relatively higher pH_{pzc} values. However, the crystalline $CuFe_2O_4$ illustrates a lower pH_{pzc} value, which is consistent with previously reported values (Zhang T et al., 2013; Tu et al., 2014; Sun et al., 2015). For the FC1, a remarkable decrease in pH_{pzc} value has been observed after reaction with As(V) and the pH_{pzc} of As(V)-adsorbed FC1 is about 6.7. Apparently, As (V) is specifically adsorbed by the FC1, since the specific sorption of anions leads to a shift of the pH_{pzc} of adsorbent to a lower pH value (Hsia et al., 1999; Ren et al., 2011). However, a slight decrease in pH_{pzc} of FC1 has been found after reaction with As(III). Commonly, the adsorption of uncharged As(III) species can not result a significant shift in pH_{pzc} of adsorbents (Ren et al., 2011). The slight decrease in pH_{pzc} might be explained as follows. A small part of As (III) adsorbed on the FC1 was oxidized to As(V) by the dissolved oxygen because the experiments were conducted in an open system and the present CuO content might catalyze this reaction. For the FC2, FC3 and FC4, similar phenomena have been observed.

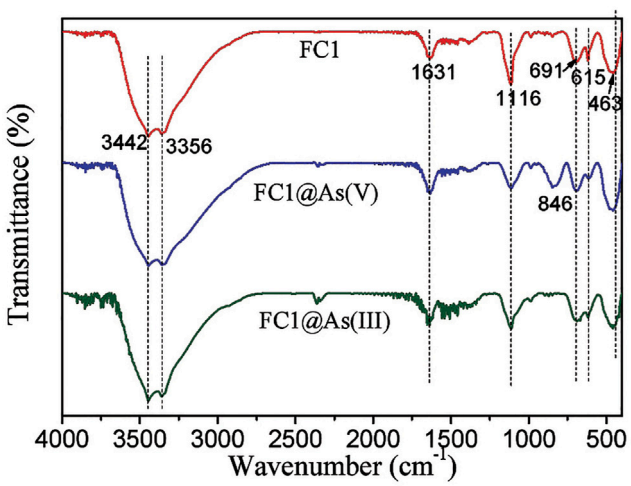

FIGURE 8 | FTIR spectra of Fe-Cu binary oxides before and after arsenic adsorption. Initial arsenic concentration = 10 mg/L, adsorbent dose = 200 mg/L, pH = 7.0 ± 0.1.

FTIR spectra of the FC1 before and after arsenic adsorption are depicted in **Figure 8**. For the pristine FC1, the peaks at 3,442

and 3,356 cm^{-1} may belong to the vibration of O-H stretching and the peak at 1,631 cm^{-1} may be ascribed to the deformation vibration of water molecules, implying that the surface of FC1 sorbed water molecules through physical adsorption; the peak at 1,116 cm^{-1} may be assigned to the vibration of SO_4^{2-} (Lefevre, 2004); the three peaks at 691, 615 and 463 cm^{-1} may be ascribed to the overlap of the HO- deformation vibration of ferrihydrite and Cu–O stretching (Kliche and Popovic, 1990). After As (V) adsorption, the intensity of peak at 1,116 cm^{-1} weakens and a new peak appears at 846 cm^{-1}, which may be due to the vibration (As-OH) of As-O-M groups (Goldberg and Johnston, 2001). This result suggests that the As (V) is mainly sorbed through the formation of inner-sphere surface complexes. While no significant change has been observed after As (III) adsorption. Similar phenomena were also observed for arsenic adsorption by other metal oxides (Ren et al., 2011).

Based on the analyses of zeta potentials and FTIR sepctra, it could be reasonably concluded that the As (V) is specifically sorbed by the FCBOs via formation of inner-sphere surface complexes, while As (III) is sorbed through formation of both inner- and outer-sphere surface complexes.

CONCLUSION

A series of Fe-Cu binary oxides were prepared under different solution pH values. The crystallinity and saturation magnetization of prepared Fe-Cu binary oxide increased with an increase in synthetic pH value. Simultaneously, the morphology of FCBO changed gradually from irregular agglomerate to relatively uniform polyhedron. The adsorption of arsenic on FCBOs is remarkably affected by the surface structure and crystallinity, decreasing as the degree of crystallinity increases. Surface hydroxyl density of FCBOs is an important parameter to evaluate its arsenic adsorption ability. Nevertheless, the adsorption ability may be overestimated if only this parameter is used. As (V) is sorbed by the FCBOs via formation of inner-sphere surface complexes and As (III) is sorbed through formation of both inner- and outer-sphere surface complexes. This investigation provides new insights into structure-performance relationship of FCBOs system, which are beneficial to develop new and efficient sorbents. However, the characterization of FCBOs is still not insufficient in this study and more powerful techniques such as X-Ray Absorption Fine Structure (XAFS) are needed to reveal further the structure-performance relationship of FCBOs system in future study.

DATA AVAILABILITY STATEMENT

The original contributions presented in the study are included in the article/**Supplementary Material** further inquiries can be directed to the corresponding authors.

AUTHOR CONTRIBUTIONS

GZ: Conceptualization, Writing—Original draft preparation. ZW: Investigation, Formal analysis. QQ: Investigation. YW: Conceptualization, Writing—Reviewing and Editing.

ACKNOWLEDGMENTS

The authors acknowledge financial support by Guangzhou Science and Technology Project (202102010385) and Rural Revitalization Strategy Project from the Department of Science and Technology of Guangdong Province(620096-3).

SUPPLEMENTARY MATERIAL

The Supplementary Material for this article can be found online at: https://www.frontiersin.org/articles/10.3389/fchem.2021.840446/full#supplementary-material

REFERENCES

Anandan, S., Selvamani, T., Prasad, G. G., M. Asiri, A. A., and J. Wu, J. (2017). Magnetic and Catalytic Properties of Inverse Spinel $CuFe_2O_4$ Nanoparticles. *J. Magnetism Magn. Mater.* 432, 437–443. doi:10.1016/j.jmmm.2017.02.026

Antelo, J., Fiol, S., Pérez, C., Mariño, S., Arce, F., Gondar, D., et al. (2010). Analysis of Phosphate Adsorption onto Ferrihydrite Using the CD-MUSIC Model. *J. Colloid Interf. Sci.* 347 (1), 112–119. doi:10.1016/j.jcis.2010.03.020

Chen, J., Wang, J., Zhang, G., Wu, Q., and Wang, D. (2018). Facile Fabrication of Nanostructured Cerium-Manganese Binary Oxide for Enhanced Arsenite Removal from Water. *Chem. Eng. J.* 334, 1518–1526. doi:10.1016/j.cej.2017.11.062

Cui, H., Li, Q., Gao, S., and Shang, J. K. (2012). Strong Adsorption of Arsenic Species by Amorphous Zirconium Oxide Nanoparticles. *J. Ind. Eng. Chem.* 18 (4), 1418–1427. doi:10.1016/j.jiec.2012.01.045

Dou, X., Li, Y., Mohan, D., Pittman, C. U., and Hu, M. (2016). A Property-Performance Correlation and Mass Transfer Study of As(v) Adsorption on Three Mesoporous Aluminas. *RSC Adv.* 6 (84), 80630–80639. doi:10.1039/c6ra14408j

Dou, X., Wang, G.-C., Zhu, M., Liu, F., Li, W., Mohan, D., et al. (2018). Identification of Fe and Zr Oxide Phases in an Iron-Zirconium Binary Oxide and Arsenate Complexes Adsorbed onto Their Surfaces. *J. Hazard. Mater.* 353, 340–347. doi:10.1016/j.jhazmat.2018.04.004

Goldberg, S., and Johnston, C. T. (2001). Mechanisms of Arsenic Adsorption on Amorphous Oxides Evaluated Using Macroscopic Measurements, Vibrational Spectroscopy, and Surface Complexation Modeling. *J. Colloid Interf. Sci.* 234, 204–216. doi:10.1006/jcis.2000.7295

Guan, X., Du, J., Meng, X., Sun, Y., Sun, B., and Hu, Q. (2012). Application of Titanium Dioxide in Arsenic Removal from Water: A Review. *J. Hazard. Mater.* 215-216, 1–16. doi:10.1016/j.jhazmat.2012.02.069

Han, C., Li, H., Pu, H., Yu, H., Deng, L., Huang, S., et al. (2013). Synthesis and Characterization of Mesoporous Alumina and Their Performances for Removing Arsenic(V). *Chem. Eng. J.* 217, 1–9. doi:10.1016/j.cej.2012.11.087

Hofmann, A., Pelletier, M., Michot, L., Stradner, A., Schurtenberger, P., and Kretzschmar, R. (2004). Characterization of the Pores in Hydrous Ferric Oxide Aggregates Formed by Freezing and Thawing. *J. Colloid Interf. Sci.* 271, 163–173. doi:10.1016/j.jcis.2003.11.053

Hristovski, K. D., Westerhoff, P. K., Crittenden, J. C., and Olson, L. W. (2008). Arsenate Removal by Nanostructured ZrO_2 Spheres. *Environ. Sci. Technol.* 42 (10), 3786–3790. doi:10.1021/es702952p

Hsia, T.-H., Lo, S.-L., Lin, C.-F., and Lee, D.-Y. (1994). Characterization of Arsenate Adsorption on Hydrous Iron Oxide Using Chemical and Physical Methods. *Colloids Surf. A: Physicochem. Eng. Aspects* 85, 1–7. doi:10.1016/0927-7757(94)02752-8

Hu, X., Ding, Z., Zimmerman, A. R., Wang, S., and Gao, B. (2015). Batch and Column Sorption of Arsenic onto Iron-Impregnated Biochar Synthesized through Hydrolysis. *Water Res.* 68, 206–216. doi:10.1016/j.watres.2014.10.009

Jegadeesan, G., Al-Abed, S. R., Sundaram, V., Choi, H., Scheckel, K. G., and Dionysiou, D. D. (2010). Arsenic Sorption on TiO_2 Nanoparticles: Size and Crystallinity Effects. *Water Res.* 44 (3), 965–973. doi:10.1016/j.watres.2009.10.047

Jordan, N., Ritter, A., Scheinost, A. C., Weiss, S., Schild, D., and Hübner, R. (2014). Selenium(IV) Uptake by Maghemite (γ-Fe2O3). *Environ. Sci. Technol.* 48 (3), 1665–1674. doi:10.1021/es4045852

Kliche, G., and Popovic, Z. V. (1990). Far-infrared Spectroscopic Investigations on CuO. *Phys. Rev. B* 42, 10060–10066. doi:10.1103/physrevb.42.10060

Kosmulski, M. (2009). Compilation of PZC and IEP of Sparingly Soluble Metal Oxides and Hydroxides from Literature. *Adv. Colloid Interf. Sci* 152 (1), 14–25. doi:10.1016/j.cis.2009.08.003

Lefèvre, G. (2004). *In Situ* fourier-transform Infrared Spectroscopy Studies of Inorganic Ions Adsorption on Metal Oxides and Hydroxides. *Adv. Colloid Interf. Sci.* 107, 109–123. doi:10.1016/j.cis.2003.11.002

Li, R., Li, Q., Gao, S., and Shang, J. K. (2012). Exceptional Arsenic Adsorption Performance of Hydrous Cerium Oxide Nanoparticles: Part A. Adsorption Capacity and Mechanism. *Chem. Eng. J.* 185-186, 127–135. doi:10.1016/j.cej.2012.01.061

Martinson, C. A., and Reddy, K. J. (2009). Adsorption of Arsenic(III) and Arsenic(V) by Cupric Oxide Nanoparticles. *J. Colloid Interf. Sci.* 336 (2), 406–411. doi:10.1016/j.jcis.2009.04.075

Mertens, J., Rose, J., Wehrli, B., and Furrer, G. (2016). Arsenate Uptake by Al Nanoclusters and Other Al-Based Sorbents during Water Treatment. *Water Res.* 88, 844–851. doi:10.1016/j.watres.2015.11.018

Mohan, D., and Pittman, C. U. (2007). Arsenic Removal from Water/wastewater Using Adsorbents--A Critical Review. *J. Hazard. Mater.* 142 (1), 1–53. doi:10.1016/j.jhazmat.2007.01.006

Nasir, A. M., Goh, P. S., and Ismail, A. F. (2018). Novel Synergistic Hydrous Iron-Nickel-Manganese (HINM) Trimetal Oxide for Hazardous Arsenite Removal. *Chemosphere* 200, 504–512. doi:10.1016/j.chemosphere.2018.02.126

Rao, P., Sun, Z., Zhang, W., Yao, W., Wang, L., and Ding, G. (2015). Preparation and Application of Amorphous Fe-Ti Bimetal Oxides for Arsenic Removal. *RSC Adv.* 5 (109), 89545–89551. doi:10.1039/c5ra12039j

Reddy, K. J., McDonald, K. J., and King, H. (2013). A Novel Arsenic Removal Process for Water Using Cupric Oxide Nanoparticles. *J. Colloid Interf. Sci.* 397, 96–102. doi:10.1016/j.jcis.2013.01.041

Ren, Z., Zhang, G., and Paul Chen, J. (2011). Adsorptive Removal of Arsenic from Water by an Iron-Zirconium Binary Oxide Adsorbent. *J. Colloid Interf. Sci.* 358 (1), 230–237. doi:10.1016/j.jcis.2011.01.013

Shehzad, K., Ahmad, M., Xie, C., Zhan, D., Wang, W., Li, Z., et al. (2019). Mesoporous Zirconia Nanostructures (MZN) for Adsorption of As(III) and As(V) from Aqueous Solutions. *J. Hazard. Mater.* 373, 75–84. doi:10.1016/j.jhazmat.2019.01.021

Smedley, P. L., and Kinniburgh, D. G. (2002). A Review of the Source, Behaviour and Distribution of Arsenic in Natural Waters. *Appl. Geochem.* 17 (5), 517–568. doi:10.1016/s0883-2927(02)00018-5

Sowers, T. D., Harrington, J. M., Polizzotto, M. L., and Duckworth, O. W. (2017). Sorption of Arsenic to Biogenic Iron (Oxyhydr)oxides Produced in Circumneutral Environments. *Geochim. Cosmochim. Acta* 198, 194–207. doi:10.1016/j.gca.2016.10.049

Srivastava, R. (2010). Eco-friendly and Morphologically-Controlled Synthesis of Porous CeO_2 Microstructure and its Application in Water Purification. *J. Colloid Interf. Sci.* 348 (2), 600–607. doi:10.1016/j.jcis.2010.04.076

Sun, W., Pan, W., Wang, F., and Xu, N. (2015). Removal of Se(IV) and Se(VI) by MFe_2O_4 Nanoparticles from Aqueous Solution. *Chem. Eng. J.* 273, 353–362. doi:10.1016/j.cej.2015.03.061

Tamura, H., Tanaka, A., Mita, K.-Y., and Furuichi, R. (1999). Surface Hydroxyl Site Densities on Metal Oxides as a Measure for the Ion-Exchange Capacity. *J. Colloid Interf. Sci.* 209 (1), 225–231. doi:10.1006/jcis.1998.5877

Tu, Y.-J., You, C.-F., Chang, C.-K., Wang, S.-L., and Chan, T.-S. (2012). Arsenate Adsorption from Water Using a Novel Fabricated Copper Ferrite. *Chem. Eng. J.* 198-199, 440–448. doi:10.1016/j.cej.2012.06.006

Tu, Y.-J., You, C.-F., Chang, C.-K., Chan, T.-S., and Li, S.-H. (2014). XANES Evidence of Molybdenum Adsorption onto Novel Fabricated Nano-Magnetic $CuFe_2O_4$. *Chem. Eng. J.* 244, 343–349. doi:10.1016/j.cej.2014.01.084

Usman, M., Zarebanadkouki, M., Waseem, M., Katsoyiannis, I. A., and Ernst, M. (2020). Mathematical Modeling of Arsenic(V) Adsorption onto Iron Oxyhydroxides in an Adsorption-Submerged Membrane Hybrid System. *J. Hazard. Mater.* 400, 123221. doi:10.1016/j.jhazmat.2020.123221

Usman, M., Belkasmi, A. I., Kastoyiannis, I. A., and Ernst, M. (2021). Pre-deposited Dynamic Membrane Adsorber Formed of Microscale Conventional Iron Oxide-based Adsorbents to Remove Arsenic from Water: Application Study and Mathematical Modeling. *J. Chem. Technol. Biotechnol.* 96, 1504–1514. doi:10.1002/jctb.6728

Wei, Y., Liu, H., Liu, C., Luo, S., Liu, Y., Yu, X., et al. (2019). Fast and Efficient Removal of As(III) from Water by $CuFe_2O_4$ with Peroxymonosulfate: Effects of Oxidation and Adsorption. *Water Res.* 150, 182–190. doi:10.1016/j.watres.2018.11.069

Yan, L., Huang, Y., Cui, J., and Jing, C. (2015). Simultaneous As(III) and Cd Removal from Copper Smelting Wastewater Using Granular TiO_2 Columns. *Water Res.* 68, 572–579. doi:10.1016/j.watres.2014.10.042

Yu, X.-Y., Xu, R.-X., Gao, C., Luo, T., Jia, Y., Liu, J.-H., et al. (2012). Novel 3D Hierarchical Cotton-candy-like CuO: Surfactant-free Solvothermal Synthesis and Application in As(III) Removal. *ACS Appl. Mater. Inter.* 4 (4), 1954–1962. doi:10.1021/am201663d

Zhang, G., Liu, F., Liu, H., Qu, J., and Liu, R. (2014). Respective Role of Fe and Mn Oxide Contents for Arsenic Sorption in Iron and Manganese Binary Oxide: An X-ray Absorption Spectroscopy Investigation. *Environ. Sci. Technol.* 48 (17), 10316–10322. doi:10.1021/es501527c

Zhang, G., Liu, Y., Wang, J., and Li, H. (2020). Efficient Arsenic(III) Removal from Aqueous Solution by a Novel Nanostructured Iron-Copper-Manganese Trimetal Oxide. *J. Mol. Liquids* 309, 112993. doi:10.1016/j.molliq.2020.112993

Zhang G, G., Ren, Z., Zhang, X., and Chen, J. (2013). Nanostructured Iron(III)-Copper(II) Binary Oxide: A Novel Adsorbent for Enhanced Arsenic Removal from Aqueous Solutions. *Water Res.* 47 (12), 4022–4031. doi:10.1016/j.watres.2012.11.059

Zhang T, T., Zhu, H., and Croué, J.-P. (2013). Production of Sulfate Radical from Peroxymonosulfate Induced by a Magnetically Separable $CuFe_2O_4$ Spinel in Water: Efficiency, Stability, and Mechanism. *Environ. Sci. Technol.* 47 (6), 2784–2791. doi:10.1021/es304721g

Conflict of Interest: The authors declare that the research was conducted in the absence of any commercial or financial relationships that could be construed as a potential conflict of interest.

Publisher's Note: All claims expressed in this article are solely those of the authors and do not necessarily represent those of their affiliated organizations, or those of the publisher, the editors and the reviewers. Any product that may be evaluated in this article, or claim that may be made by its manufacturer, is not guaranteed or endorsed by the publisher.